Hindawi
Advances in Civil Engineering
Volume 2022, Article ID 5858400, 15 pages
https://doi.org/10.1155/2022/5858400

Research Article

Rainfall & Seismological Dump Slope Stability Analysis on Active Mine Waste Dump Slope with UAV

Shirshendu Layek, Vasanta Govind Kumar Villuri, Radhakanta Koner, and Kapoor Chand

Department of Mining Engineering, Indian Institute of Technology (ISM), Dhanbad 826004, India

Correspondence should be addressed to Shirshendu Layek; shirshendu@me.ism.ac.in and Vasanta Govind Kumar Villuri; vgkvilluri@iitism.ac.in

Received 25 February 2022; Revised 26 May 2022; Accepted 17 June 2022; Published 12 August 2022

Academic Editor: Kamal Jain

Mine waste dump material has no economic value to the industry. Therefore, the mine waste is dumped, forming slopes. Mine waste dump slopes obtain 30% to 50% of the mining area. To reduce the land occupancy of these slopes, they are created with high altitudes. Hence, they are susceptible to failure. Slope stability analysis is a major aspect of geotechnical engineering. Slope stability analyses are mostly done with assumptions on the geometry. This is avoided in this paper with the usage of UAVs. The 3D model is created from UAV imagery of a coal mine in Raniganj coalfield, India. The model is fine-tuned with the DGPS survey. Geotechnical data were collected and tested in the laboratory for various numerical analyses. An active mine waste dump slope is analyzed for slope failure. Earthquakes and rainfall cannot be controlled, and their effects on the stability of the mine waste dump slope were examined. The study extracted various factor of safety (FOS) analyses on static, seismic, and rainfall conditions. The seismic condition simulates a condition of the slope to be failed with low (0.948) FOS. However, rainfall condition predicts the slope to be more stable. The deformation pattern and magnitude of the slope failure are also discussed.

1. Introduction

Open-pit mining operation excavates the top portion of the soil to extract minerals or coals. During this process, the excavated soil had no economic value to the mining industry. These materials are known as waste [1, 2]. The limitation of the mining area makes it tedious to manage this waste. Therefore, the mine waste is dumped, forming a slope [3, 4]. These dump slopes are enormous. Mine waste dump is made very rapidly, therefore less time for consolidation of waste materials. This hasty approach is making the slopes susceptible to form disasters. From 1921, there were 23 accidents due to mine overburden slope failures only in India. These accidents cost 143 causalities [5, 6]. In 2016, a catastrophic slope failure in Rajmahal opencast mine caused the death of 23 people. Talcher, Bokaro, and Bharatpur recently faced similar accidents [7–9]. Mine dump slope stability analysis is a major subject in geotechnical engineering. The safety study is based on these slopes with SSR (Shear Strength Reduction). In this technique, soil material's strength characteristics are reduced till the failure is obtained in the geometry [10]. This method provides a numeric value that represents the factor of safety [11]. If the value is greater than one, then the stability of the slope is high and vice-versa [12–15]. For traditional numerical simulation, an assumption on geometry is considered [16]. With the usage of UAV, two significant problems in numerical simulations can be solved, the first reduction in geometry assumption, and the second, the GIS tools can be used for mapping, monitoring, and targeting the risk-prone areas for numerical simulation resulting in accurate analysis and less computational time. This approach is possible with UAV's RGB (red, green, and blue) imagery. Overlapped images of UAVs can create a 3D point cloud of an area [17–19]. Furthermore, DTM for slope targeting for

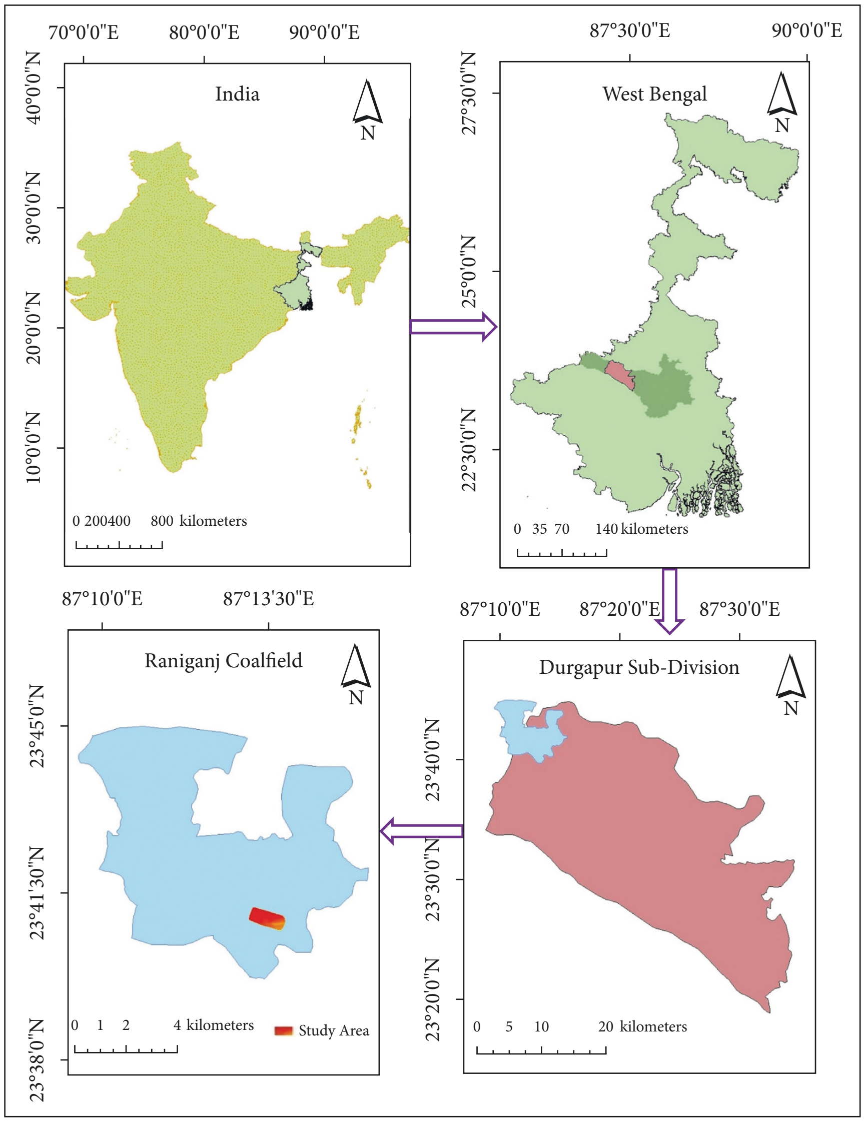

Figure 1: Map showing the study area, located in India's eastern part.

numerical simulation and geometry for numerical simulation can be developed. For testing this approach, Raniganj coalfield, India, has been selected (Figure 1 represents the study area). Raniganj is situated in the eastern part of India. This coalfield region is about 1130 km^2 from 23°25′N to 23°50′N latitude and 86°38′E to 87°20′E longitude [20].

Raniganj coal mines have most of the open cast projects of Eastern Coalfield Ltd., India. In Raniganj coalfield, the biggest open cast mine is situated in Sonepure Bazari [2]. The production of the coalfield is 33.90 million tonnes; thus, high mining activity occurs consistently. The mine we selected has an in-pit waste dumping system, i.e., waste is dumped within the mining area due to the limited range of available land. In-pit waste dump of the study area is shown in Figure 2.

An active mine dumping area was taken for testing for stability analysis, as the chances of failure will be high due to less time for waste to consolidate [12]. Hence, traditional numerical simulation is insufficient in this scenario as rainfall plays a vital role in slope failures and earthquakes [21]. As Raniganj is a subtropical place, heavy rain occurs, and precipitation of 200 to 400 mm every monsoon has been reported yearly. Also, regular cyclones have been impeding [22]. Therefore, an increase in rain directly affects the safety factor of the overburden slope [23].

Figure 2: In-pit mining waste dump at the study area.

2. Materials and Methods

This study focuses on the stability analysis of the active in-pit mine waste dump. Therefore, in data acquisition, UAV imagery, DGPS survey, and geotechnical samples were collected from the study area. With the help of UAV imagery,

3D modeling and proper geometry are extracted from the active waste dump slope. The area was cross-checked with GIS to ensure the proneness to failure. Finally, three geometry of the section was extracted, and numerical simulations were done with the help of geotechnical data. In Figure 3, the steps can be followed. There are four steps to achieving the desired goal; data collection, geotechnical analysis, image processing, and numerical simulation. The numerical simulation focuses on rainfall effects on the stability of the slope and the simulation of seismological impact on the slope. These parts are discussed in this section.

2.1. UAV Data Acquisition. In the field, DJI Phantom 4 Pro UAV has been used (Figure 4 shows the UAV). The UAV can fly for up to 19 minutes on a single charge and capture 20-megapixel resolution worth of imagery. Acquisition of images is made with overlapping of 75% in horizontal and 65% in vertical. DGPS (differential global positioning system) was also used for the accuracy of the generated model [24–26].

The average GSD of the constructed orthoimagery was 5.022 cm per pixel. A total of 561 images were captured with two flights. And the flight plan was grid in nature. The area captured by the UAV is 4716900 m^2. DGPS can extract coordinates of an unknown area without reference. Prominent "+" symbols were drawn in the field with whitewash for this study, as shown in Figure 5. Seven GCPs were used to process the images in Pix4DMapper. As per the software Pix4DMapper with seven GCPs, the RMS should be less than 0.10, making the model highly accurate.

The overlapping helps in recovering lost 3D information of the camera with the same feature extraction in multiple images, and triangulation is done to retrieve the position of the camera in x, y, and z coordinates by reversing the approach after extracting camera location, x, y, and z coordinates of features are extracted. This approach is made by structure from motion pipeline for generating 3D point cloud and other forms of data [27, 28].

2.2. Geotechnical Analysis. Accurate shear strength parameters, i.e., cohesion and internal frictional angle of the waste materials, are necessary for numerical simulation accuracy [29, 30], along with those compaction characteristics that are also needed. For shear strength parameters, triaxial tests were performed [31], and compaction tests were carried out according to Indian Standard (IS:2720) part-6 (1965). Hence, a geotechnical investigation was necessary. The materials were initially tested with grain size distribution. According to Indian Standard Soil Classification System (ISSCS) with various tests, the material showed coarse materials between 80% and 98%, and sand between 2 mm and 0.425 mm was ranging from 22% to 92% and, sand and clay ranging from 3.8% to 46% (particles are less than 0.75 mm) thus making the material poorly graded sand or SP. The samples were collected during UAV data acquisition and have been processed in the institute's laboratory facilities, and the extracted geotechnical parameters can be seen in Table 1.

2.3. 3D Model of UAV Imagery. 3D modeling from UAV imagery is based on epipolar geometry of photogrammetry [28, 32]. Therefore, feature extraction and matching of multiple images are done. Matched features of image pairs are used to create pose estimation (3D location of the camera of the same feature found in various images) with triangulation hence, spatial 3D point cloud data [33, 34]. To minimize errors, bundle adjustment is applied. Bundle adjustment is used on the accumulated 3D model to refine and prevent noise in triangulation [35]. This model is created from a UAV. This 3D model, along with an orthomosaicked image, was used to create a digital elevation model (DEM) for inspection of AOI.

Furthermore, to be accurate, the geometry DGPS surveyed data were integrated before processing the 3D point cloud as ground control points in Pix4DMapper. Figure 6 shows the 3D model of the study area, which is generated from UAV imagery.

2.4. Geometry Extraction for Numerical Analysis. The surveyed area from the UAV mainly covered the mining dump, but most of the area was not visible from the ground survey or observation. So, removing fewer risk-prone zones from the surveyed area helps reduce computational time. The authors targeted an active waste dump slope to be examined. A newly made dump has less time to settle down, and having loose materials causes low shear strength. Therefore, failure can occur.

In Figure 7, the active dumping zone is shown. This area initially needs to be examined with GIS. The GIS technology can cross-check whether the active dumping slope is prone to failure. This is done by developing a slope map of the study area from UAV data. Slope angles represent the relative angle displacements. In Figure 8, the slope map is shown.

From Figure 8, it can be seen that the angular value of the targeted zone exceeds 36 degrees. Thus, this site makes it ideal for examining numerical simulation for slope stability.

Three sections from the active dumping zone have been extracted. These geometries can be seen in Figures 9(b)–9(d). The geometries from the same dumping slope have different angles and heights. Examining only one will derive less in-depth analysis. These sections have a length of 207, 210, and 198 meters horizontally and 66, 83, and 101 meters in altitude displacement (the projection in the figure is in 3D; hence, the perspective of displacement on different axis differs).

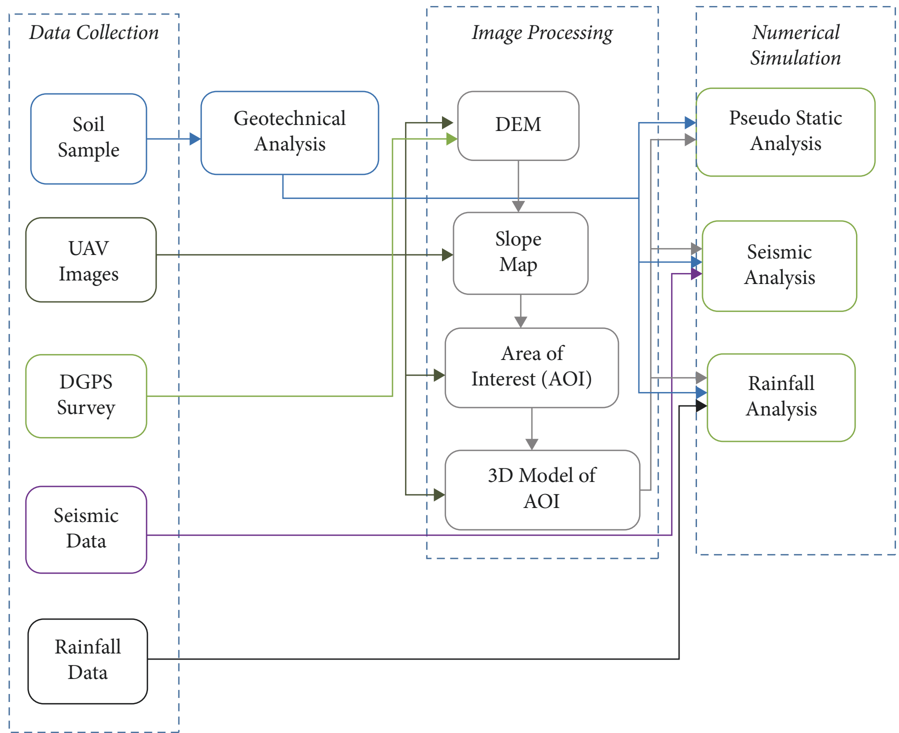

Figure 3: Slope stability analysis method in static, seismic, and rainfall conditions with the UAV.

Figure 4: UAV data acquisition in the study area.

3. Results and Discussion

Flac comes with computing packages for numerical simulation applications. This is widely accepted and recognized. In Flac3D, numerical analysis is done with the shear strength reduction technique or SSR. Constraint boundaries restrict developed geometries. This approach improves accuracy, efficiency, and modeling time, ensuring accuracy and legitimacy [36, 37]. Three geometries were extracted from the targeted waste dump slope. These geometries range between 66 meters and 101 meters in height and 197 meters to 210 meters horizontally. Mohr-Coulomb's failure criteria were adopted in the first iteration of stability analysis. The failure occurs with the critical combination of the shear strength of loose mine waste dump materials with normal stress. The loose, broken waste dump materials contain low shear strength [38, 39]. The dump slope was numerically analyzed with finite element method codes, and the FOS was calculated with displacement values, as shown in Table 2.

The slope seems to be stable with low displacement values in all the scenarios [38]. Furthermore, the sliding portion of the geometries can be seen in Figure 10. All the failures are circular. The FOS of the sections ranged from 1.26 to 1.53 of the slope under static conditions.

As discussed earlier, static slope stability analysis is insufficient as two significant reasons slope failures occur due to heavy rainfall and seismological effects. These two factors cannot be dealt with human intervention. Therefore, examining these two factors will ensure a more nuanced analysis on analysis.

3.1. Pseudostatic Condition for Seismic Effect. India is divided into four zones for an earthquake. The study area of this paper has zone III in terms of earthquake hazards. According to Figure 11, the study area lies in the moderate damage risk zone, and the factor is 0.16.

A seismic load is given in the numerical simulation of the seismological effect, i.e., 0.16. Therefore, the integrity of the analysis of the limit equilibrium method [41] with seismic conditions on the geometries is ensured. The extracted FOS from the simulation validated a lower stability factor than the static condition. In Table 3 no. 3 FOS of three sections can be seen.

The seismological effect also extracted similar failure patterns as a static condition. The LEM method provides only a stability factor. Therefore, stress and strain information is not achievable, resulting in nondeformation analysis in pseudostatic conditions. The sections after numerical simulation can be seen in Figure 12.

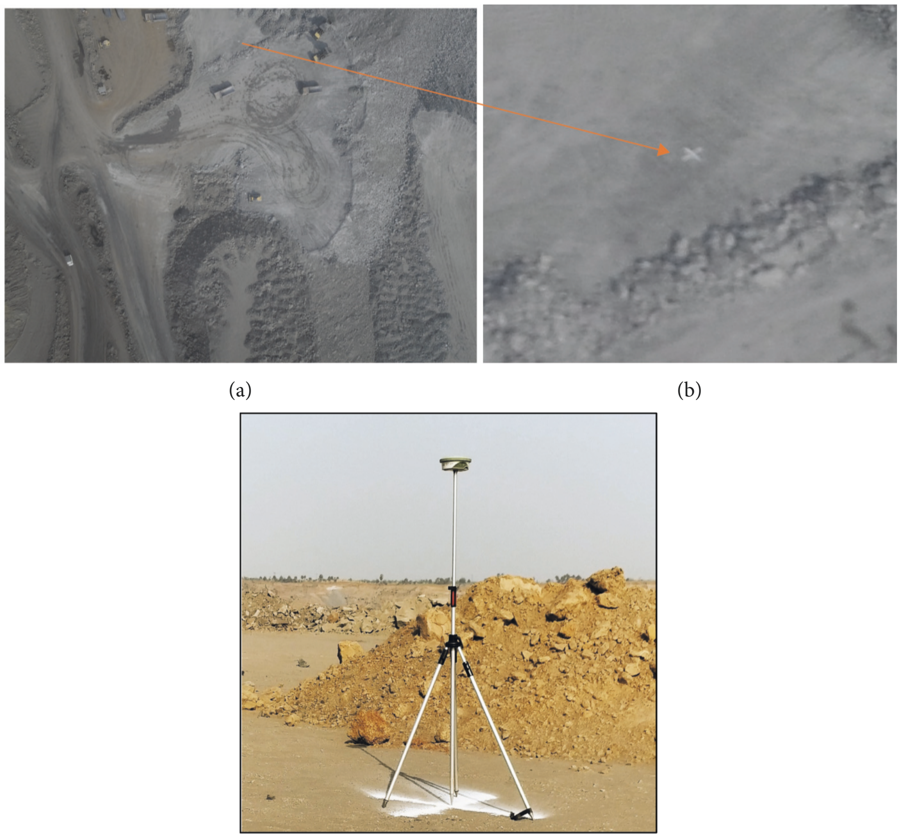

(a) (b) (c)

Figure 5: (a, b) represent temporary ground control point and (c) DGPS data acquisition for improving the accuracy of the UAV dataset.

Table 1: Waste dump material properties extracted from laboratory tests.

Parameters	Tested result
Soil unit weight (kN/m^3)	17.59914
Friction angle (degree)	25.556
Cohesion (Pa)	50000
Bulk modulus (GPa)	0.32
Shear (GPa)	3.1

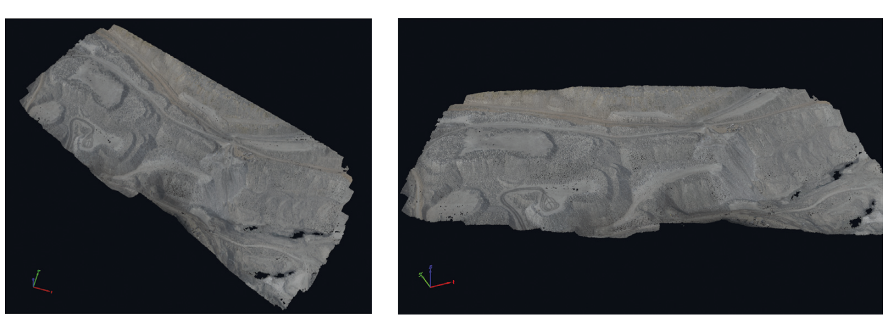

(a) (b)

Figure 6: (a, b) 3D models of the study area created from UAV imagery from different views.

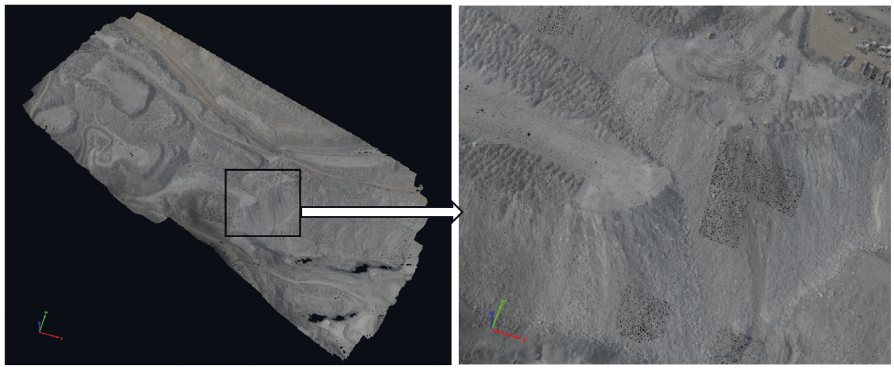

Figure 7: Active waste dumping zone in the study area.

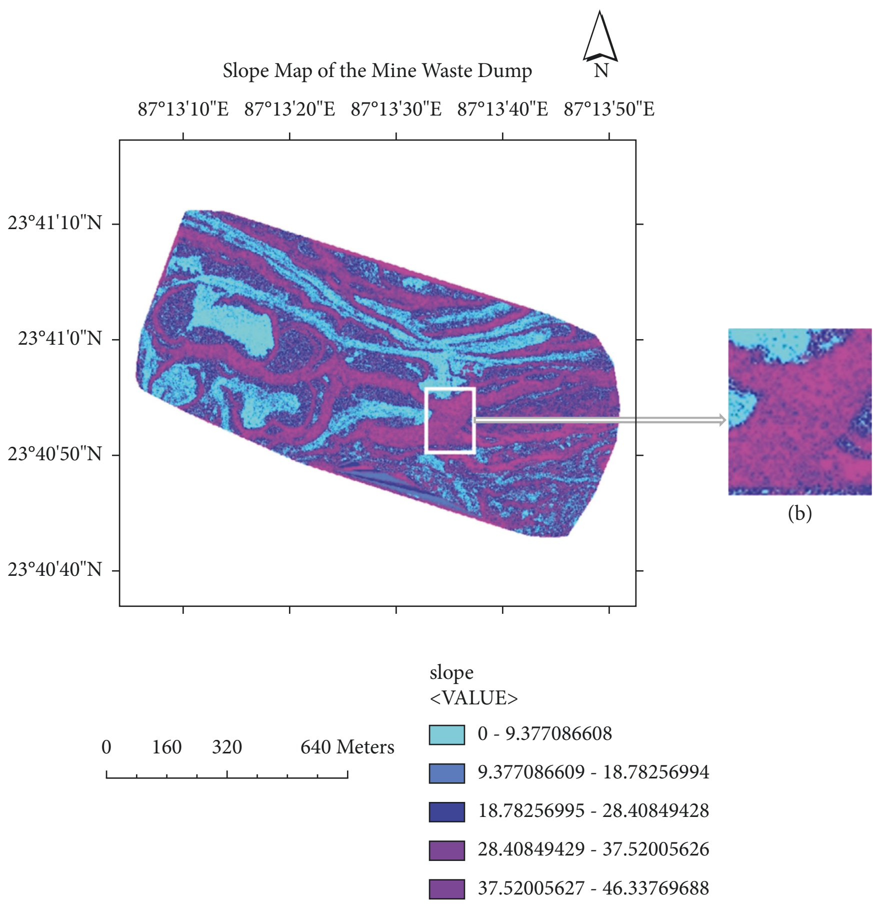

Figure 8: Slope map of the area and (b) cropped area represents the active waste dump slope.

This section validates the analysis methodology as to its capability to calculate the slope failure surface with seismic acceleration. The simulated result is documented with zone III seismic acceleration (Figure 11), which has been analyzed through widely recognized conventional Bishop's limit equilibrium methods [42]. The sections were further analyzed with a 2, 4, 6, and 8 seconds dynamic seismic load.

The el Centro dataset is adopted for input load. The given input data can be seen in Figure 13. This data propagates in the N-S direction. The pick of the acceleration is 0.3 g recorded around 2 seconds, and after 5 seconds, the acceleration gradually decreases with a low spike at 8 seconds and in around 25 seconds with 0.138 g. The displacement of the sections with dynamic load can be seen in Figure 14. In section 3 (Figure 13(e)), the displacement initially started with negative and then moved towards positive, which strongly proposes crack generation in the upper part of section 3 [43].

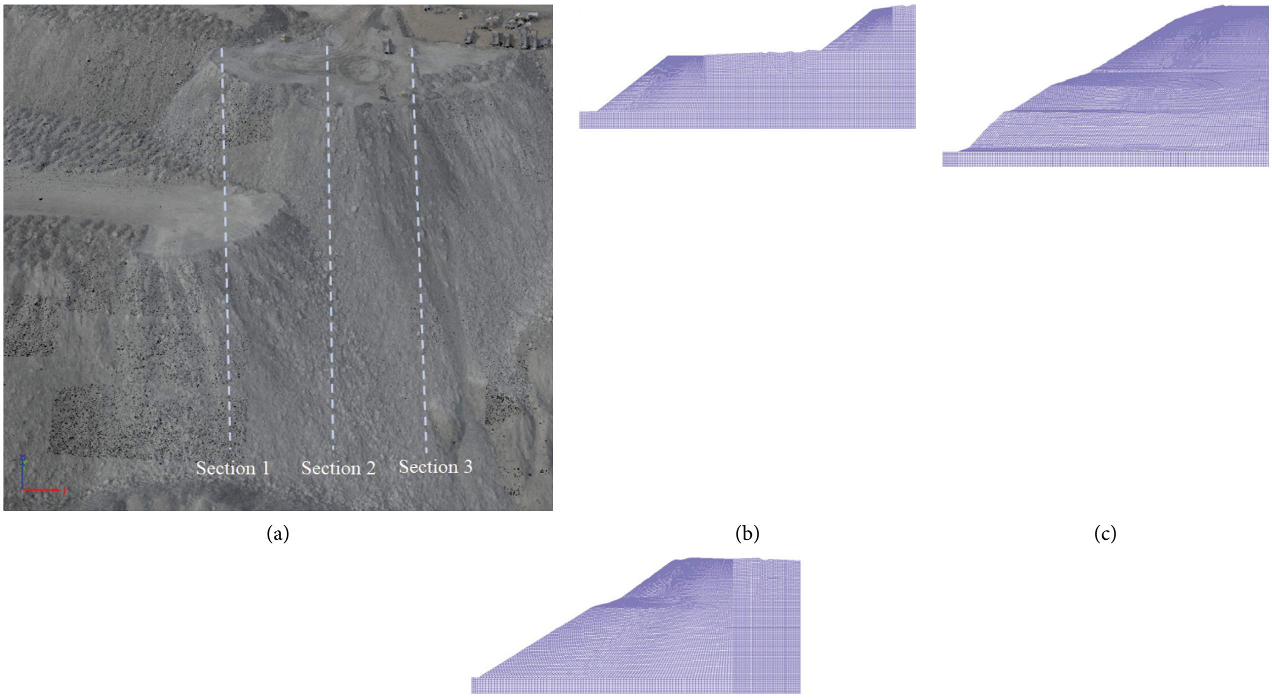

(a) (b) (c)

(d)

Figure 9: (a) Three sections marked with dotted lines on the active dumping slope. (b–d) Geometry of section 1, section 2, and section 3, respectively.

Table 2: FOS of 3 sections in static numerical simulation condition with deformation.

	FOS	Deformation (meters)
Section 1	1.53	$1.059E-01$
Section 2	1.38	$8.084E-02$
Section 3	1.26	$2.226E-01$

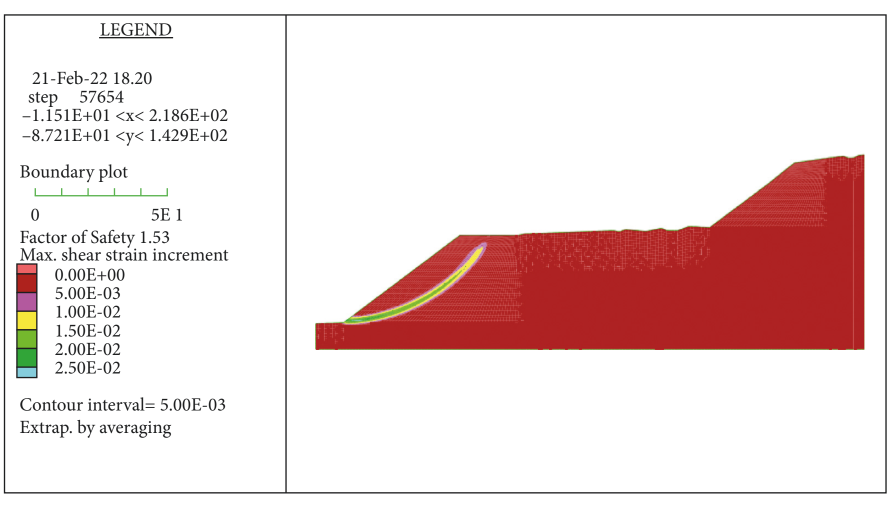

(a)

Figure 10: Continued.

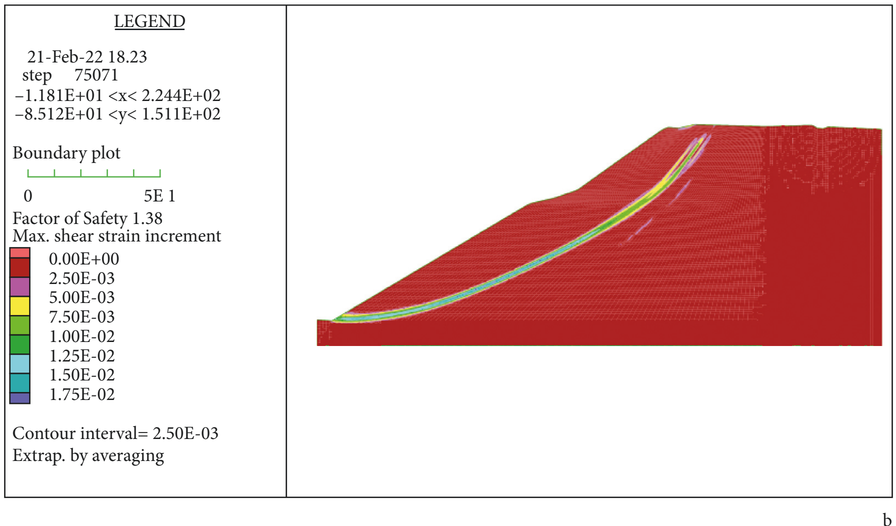

(b)

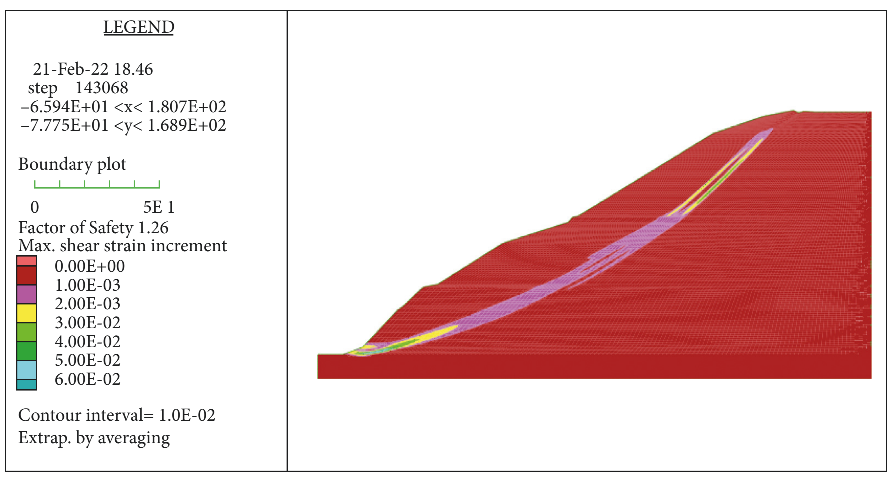

(c)

FIGURE 10: (a–c) circular failure profiles of sections 1, 2, and 3.

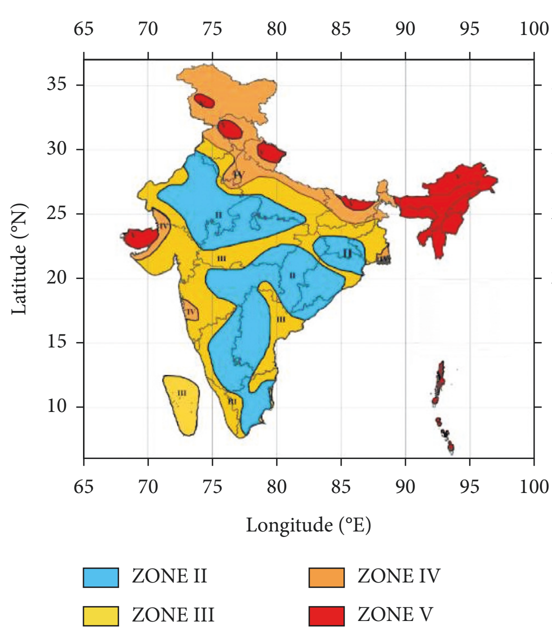

FIGURE 11: Seismological map of India [40].

Table 3: FOS after applying seismic conditions in LEM.

	FOS
Section 1	1.219
Section 2	1.048
Section 3	0.953

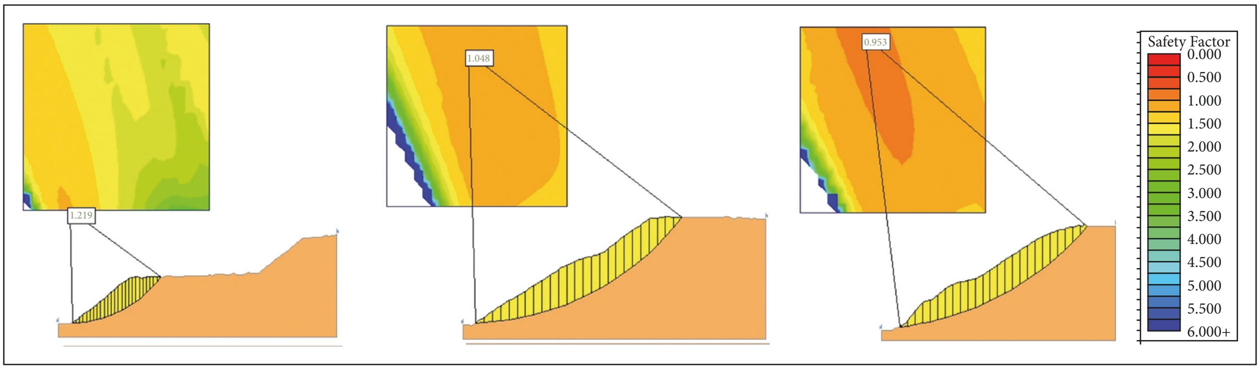

Figure 12: Pseudostatic analysis of three sections.

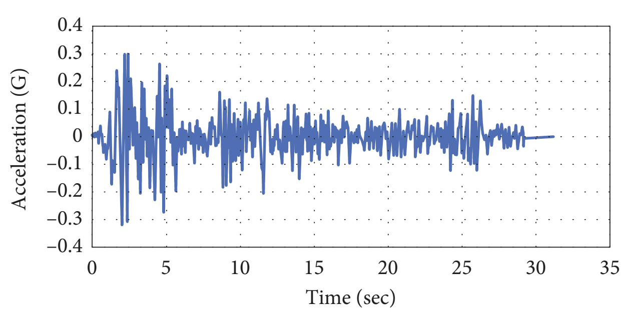

Figure 13: El centro accelerogram.

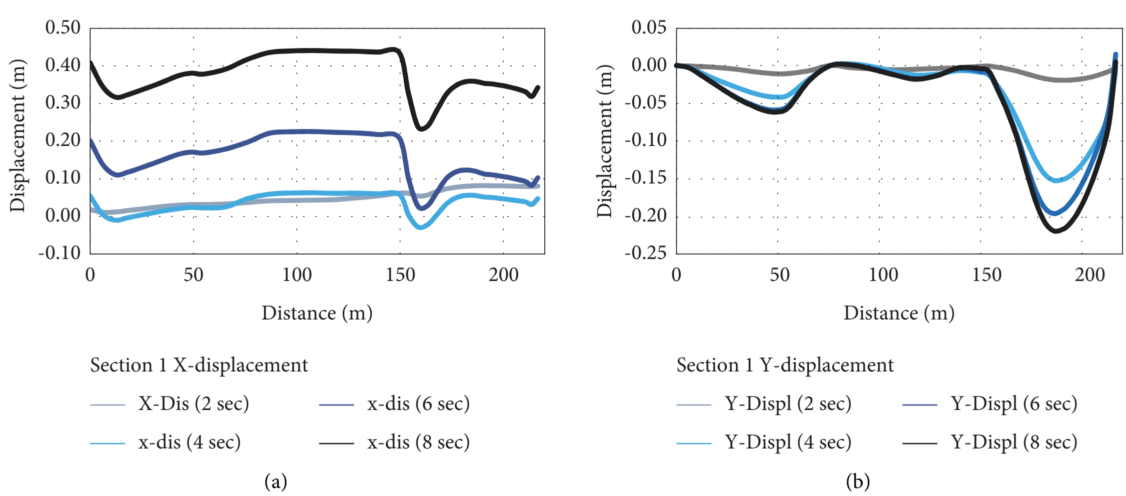

Figure 14: Continued.

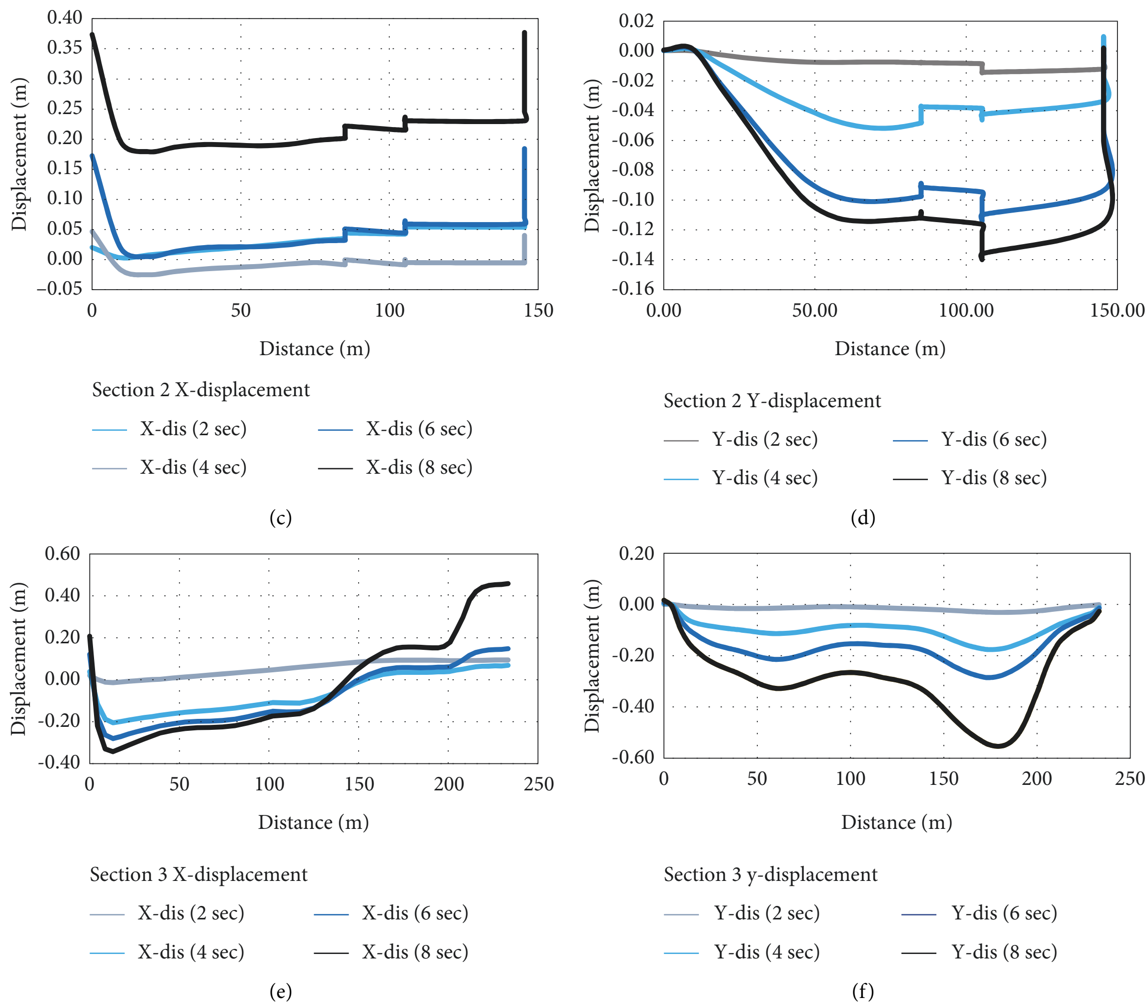

Figure 14: Dynamic load of seismic data with 2, 4, 6, and 8 seconds of sections 1, 2, and 3.

The simulation shows that the FOS of section 3 has a value of 0.953. This makes the section prone to failure. As for sections 1 and 2, they are shown a dip in FOS compared to numerical simulation in static conditions with 1.219 and 1.048.

Table 4: FOS with average rainfall during monsoon.

	FOS	Deformation (centimeters)
Section 1	1.60	7.474
Section 2	1.40	14.4
Section 3	1.25	109.8

3.2. Dump Slope Stability Analysis with Average Rainfall. The study area is subtropical in climatic nature. Hence, the rainfall occurs heavily after summer, i.e., from June to September [44–46]. Mine waste dump failures occur primarily in this period due to heavy precipitation. The precipitation in the study area was highest in August. In August, the minimum rainfall was 207.3 millimeters recorded in 2017, and the highest was in 2016 with 601.3 millimeters. In other monsoon months, precipitation varies from 28 millimeters to 515 millimeters. The average rainfall in the monsoon of the study area has been recorded as 264.266 mm in the last ten years. The numerical analysis of the study area with precipitation data was simulated for seven months. Extracted FOS can be seen in Table 4. The FOS in this scenario improved [47].

The improvement in FOS is explainable by two factors. First, seven months for settlement of the slope which is after the monsoon. The second cause is related to the waste dump material characteristic. The material contains clay that has high adhesiveness when mixed with water, which vastly improves the cohesion that benefits the bonding and stability [48]. The saturation profile of the simulation can be seen in Figure 15. This phenomenon was derived from the theory of consolidation, in which precipitation decreases the pour spaces of sand and clay-type materials and improves the consolidation with time.

Deformation of the sections stayed almost the same with low movements of the slope materials, which maxed at 1.098 meters at section 3. The displacement profile of the sections can be seen in Figure 16. The displacement on the slopes with rainfall causes less than 1 meter of negative deformation. In sections 1 and 2, the displacement goes up to 0.05 meters and

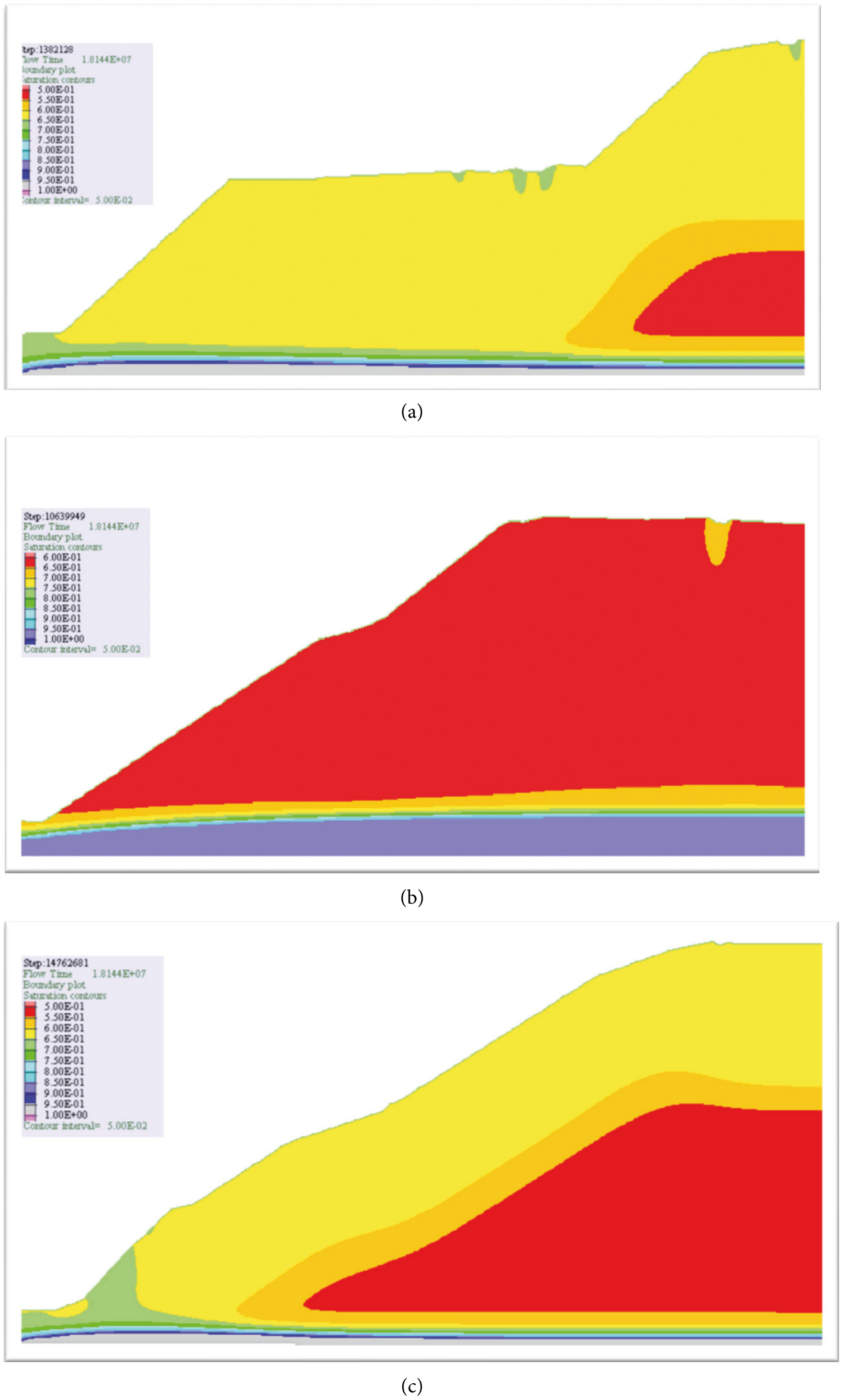

Figure 15: (a–c) represent the saturation profiles of section 1, section 2, and section 3, respectively, with a flow time of 7 months.

0.16 meters, although insection 3 geometry, the deformation goes up to 1 meter.

As a future study, rigorous analyses can be done with various FORM algorithms, and these algorithms were derived from HLRF algorithms. HLRF and FORM algorithms are known for their reliability [49, 50]. Therefore, a basic comparison of the stability of waste dump slopes can be compared with various material properties [51].

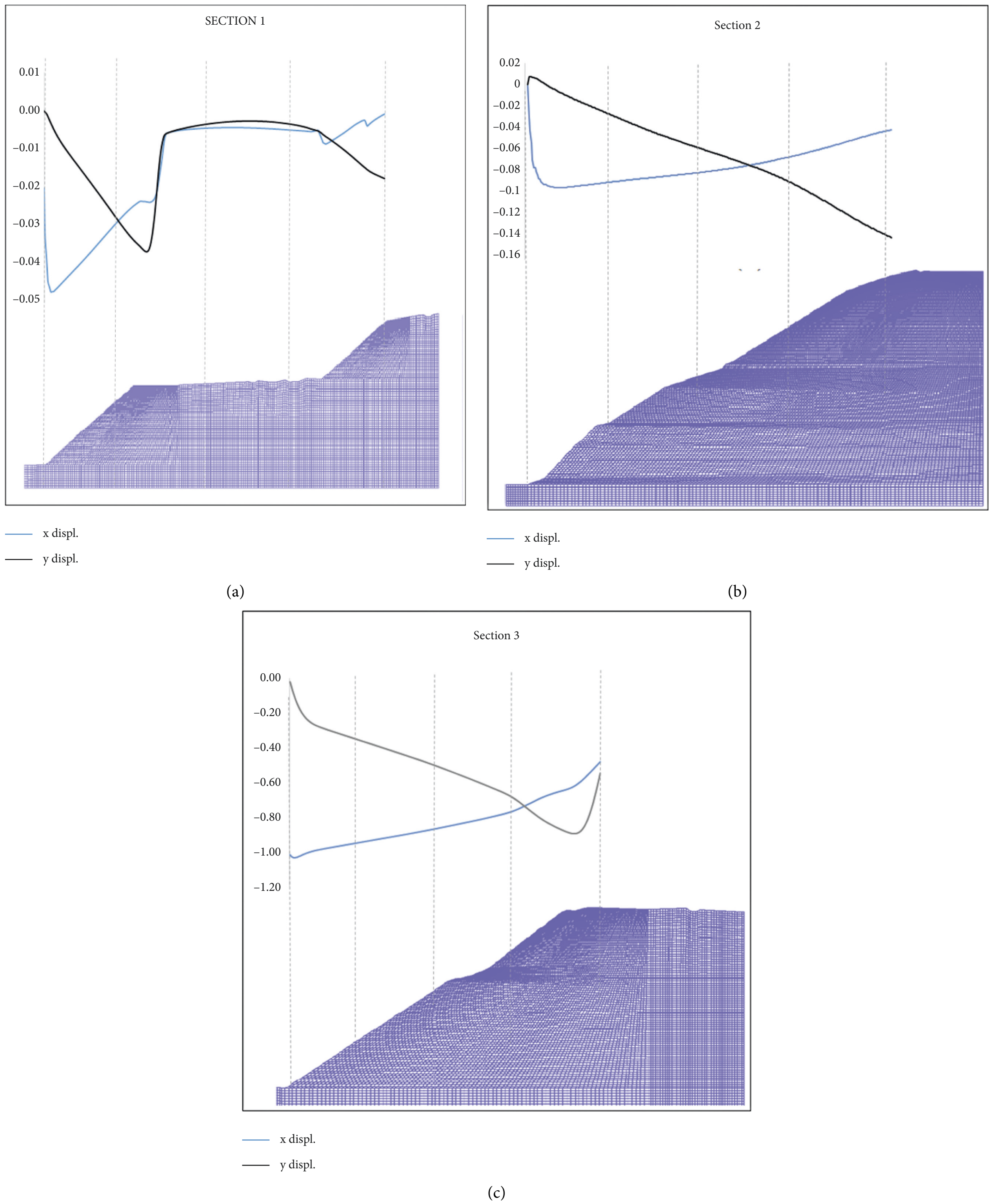

Figure 16: (a–c) represent the displacement profile in meters. The plotted displacement of the X and Y axes along the surface of the geometries of sections 1, 2, and 3 from toe to the pick of the sections.

4. Conclusions

The availability of the UAV and improvement on the image sensor is useful for creating 3D maps and models of the mining area. Proper scale and dimensions are extracted with the help of UAV imagery, DGPS, and photogrammetry. The geometries extracted from the UAV's 3D model represent an active in-pit mine dump slope, which is examined based on less time for the slope to settle waste materials. A geotechnical investigation was carried out on the dump waste materials. The geotechnical properties are instrumental in numerical analysis reliability. Numerical simulations on these geometries are carried out in three different approaches, making the study cohesive. The environments for the numerical simulation consisted of static, seismic, and rainfall conditions. These simulations show the FOS value initially at a stable state, and rainfall with seven months of simulation time increased the stability. However, the seismic condition in Bishop's limit equilibrium method shows significantly lower FOS of the sections. The least FOS was 0.948 achieved in section 3 geometry after seismic load. This outcome illustrates the failure in section 3.

Nevertheless, regular precipitation and time (or settlement of the loose materials) suggest a higher FOS, so the waste dump slope will be stable if no significant seismic acceleration occurs. The displacement analysis also indicates a maximum of 1-meter deformation. Although with seismic activity, cracks will be formed in section 3.

Data Availability

The data that support the findings of this study are available on request from the corresponding author. The data are not publicly available due to privacy or ethical restrictions.

Conflicts of Interest

The authors declare no conflicts of interest.

Acknowledgments

The research is funded by the Science and Engineering Research Board (SERB), New Delhi (Grant No - CRG/2020/005919).

References

[1] H. B. Sahu and S. Dash, "Land Degradation Due to Mining in India and its Mitigation Measures," in *Proceedings of the 2011 2nd International Conference on Environmental Science and Technology IPCBEE*, Singapore, 2011.

[2] I. Roy: Slope Stability Study of External Dump of Sonepur-Bazari Slope Stability Study of External Dump of Sonepur-Bazari Opencast Coal Mine, India-A Case Study Opencast Coal Mine, India-A Case Study SLOPE STABILITY STUDY of EXTERNAL DUMP of SONEPUR-BAZARI OPENCAST COAL MINE, INDIA-A CASE STUDY. Delhi, India, 2008.

[3] T. Gvozdkova, P. Koščová, and M. Koščová, "On the measures to solve environmental problems of the territory with intensive open pit coal mining," *E3S Web of Conferences*, vol. 105, Article ID 02006, 2019.

[4] K. Pactwa, J. Dudek, and M. Dudek, "Coal mining waste in Poland in reference to circular economy principles," *Fuel*, vol. 270, Article ID 117493, 2020.

[5] A. K. Dash, "EBSCOhost |138948870| Analysis of accidents due to slope failure in Indian opencast coal mines," 2022, https://web.p.ebscohost.com/abstract?direct=true&profile=ehost&scope=site&authtype=crawler&jrnl=00113891&AN=138948870&h=uO0Bs3%2FvzVASnZvnzdz2PLiJf5xD7QX9SjsZvQOBL%2BEchP3m6CImzVtu57%2Bppidd1AjIVmu0V1RCUbuhIP3m4Q%3D%3D&crl=c&resultNs=AdminWebAuth&resultLocal=ErrCrlNotAuth&crlhashurl=login.aspx%3Fdirect%3Dtrue%26profile%3Dehost%26scope%3Dsite%26authtype%3Dcrawler%26jrnl%3D00113891%26AN%3D138948870.

[6] M. F. Labib, A. S. Rifat, M. M. Hossain, A. K. Das, and F. Nawrine, "Road accident Analysis and Prediction of accident Severity by using machine Learning in Bangladesh," in *Proceedings of the 2019 7th Int. Conf. Smart Comput. Commun. ICSCC 2019*, Sarawak, Malaysia, June 2019.

[7] Down to Earth, "Talcher coal mine accident: 1 dead, 4 trapped after landslide," 2019, https://www.downtoearth.org.in/news/mining/talcher-coal-mine-accident-1-dead-4-trapped-after-landslide-65811.

[8] A. Abhishek, "Four trapped in Bokaro mine for over 30 hours come out safely on their own | India News,The Indian Express," 2021, https://indianexpress.com/article/india/four-trapped-in-bokaro-mine-for-over-30-hours-come-out-safely-on-their-own-7648261/.

[9] "4th body found from odisha coal mine accident site, manager suspended for negligence," 2019, https://www.news18.com/news/india/4th-body-found-from-odisha-coal-mine-accident-site-manager-suspended-for-negligence-2248703.html.

[10] H. Lu, L. Xu, and D. Fredlund, "Comparison of 3D Finite Element Slope Stability with 3D Limit Equilibrium Analysis," in *Proceedings of the 18th International Conference on Soil Mechanics and Geotechnical Engineering*, Paris, France, September 2013.

[11] X. Fu, Q. Sheng, Y. Zhang, J. Chen, S. Zhang, and Z. Zhang, "Computation of the safety factor for slope stability using discontinuous deformation analysis and the vector sum method," *Computers and Geotechnics*, vol. 92, pp. 68–76, 2017.

[12] E. M. Dawson, W. H. Roth, and A. Drescher, "Slope Stability Analysis by Strength Reduction," *Géotechnique*, vol. 49, pp. 835–840, 2015.

[13] Y. M. Cheng, T. Wei, and W. B. Wei, "Two-dimensional slope stability analysis by limit equilibrium and strength reduction methods," *Computers and Geotechnics*, vol. 34, no. 3, pp. 137–150, 2007.

[14] J. M. Duncan, "State of the art: limit equilibrium and finite-element analysis of slopes," *Journal of Geotechnical Engineering*, vol. 122, no. 7, pp. 577–596, 1996.

[15] N. Bar, M. Kostadinovski, M. Tucker et al., "Rapid and robust slope failure appraisal using aerial photogrammetry and 3D slope stability models," *International Journal of Mining Science and Technology*, vol. 30, no. 5, pp. 651–658, 2020.

[16] A. J. Li, R. S. Lyamin, and A. V. Lyamin, "Limit analysis solutions for three dimensional undrained slopes," *Computers and Geotechnics*, vol. 36, no. 8, pp. 1330–1351, 2009.

[17] S. Ullman, "The interpretation of structure from motion," *Proceedings of the Royal Society of London, Series B: Biological Sciences*, vol. 203, pp. 405–426, 1979.

[18] J. Jensen, A. Mathews, J. L. R. Jensen, and A. J. Mathews, “Assessment of image-based point cloud products to generate a bare earth surface and estimate canopy heights in a woodland ecosystem,” *Remote Sensing*, vol. 8, no. 1, p. 50, 2016.

[19] S. Layek, R. K. Singh, V. G. K. Villuri, R. Koner, A. Khare, and R. Khare, “3D reconstruction: an emerging prospect for surveying,” *Applications of Geomatics in Civil Engineering*, , pp. 71�81, Springer, Singapore, , 2020.

[20] S. Murthy, B. Chakraborti, and M. D. Roy, “Palynodating of Subsurface Sediments, Raniganj Coalfield, Damodar Basin, West Bengal,” *Journal of Earth System Science*, vol. 119, 2010.

[21] W. Du, Q. Sheng, X. Fu, J. Zhou, and Y. Zhou, “Extensions of the two-phase double-point material point method to simulate the landslide-induced surge process,” *Engineering Analysis with Boundary Elements*, vol. 133, pp. 362–375, 2021.

[22] R. S. Sannasiraj and S. A. Sannasiraj, “Climate change projection of wave climate due to Vardah cyclone in the Bay of Bengal,” *Dynamics of Atmospheres and Oceans*, vol. 97, Article ID 101279, 2022.

[23] R. Chakravarty and D. Chakravarty, “Numerical analysis of rainfall effects in external overburden dump,” *International Journal of Mining Science and Technology*, vol. 26, no. 5, pp. 825–831, 2016.

[24] C. Hoppe, M. Klopschitz, M. Donoser, and H. Bischof, “Incremental Surface Extraction from Sparse Structure-From-Motion Point Clouds,” in *Proceedings of the British Machine Vision Conference (BMVC)*, Bristol, UK, September 2013.

[25] K. Douterloigne, S. Gautama, and W. Philips, “On the accuracy of 3D landscapes from UAV image data,” in *Proceedings of the 2010 IEEE International Geoscience and Remote Sensing Symposium*, pp. 589–592, Honolulu, HI, USA, July 2010.

[26] H. Chikatsu and H. Chikatsu, “Camera calibration in 3D modelling for UAV application,” *The International Archives of the Photogrammetry, Remote Sensing and Spatial Information Sciences*, vol. XL-4/W5, pp. 223–226, 2015.

[27] M. J. Westoby, J. Brasington, N. F. Glasser, M. J. Reynolds, and J. M. Reynolds, “Structure-from-Motion’ photogrammetry: a low-cost, effective tool for geoscience applications,” *Geomorphology*, vol. 179, pp. 300–314, 2012.

[28] J. L. Schönberger and J.-M. Frahm, “Structure-from-Motion Revisited,” in *Proceedings of the 2016 IEEE Conference on Computer Vision and Pattern Recognition (CVPR)*, Las Vegas, NV, USA, June 2016.

[29] A. McQuillan, I. Oh, and J. Oh, “Methods applied in Australian industry to evaluate coal mine slope stability,” *International Journal of Mining Science and Technology*, vol. 30, no. 2, pp. 151–155, 2020.

[30] L. Zdravković and D. M. Potts, “Application of numerical analysis in geotechnical engineering practice,” *GeoFlorida*, pp. 69–88, 2010.

[31] Y. Zhou, Q. Sheng, N. Li, and X. Fu, “The dynamic mechanical properties of a hard rock under true triaxial damage-controlled dynamic cyclic loading with different loading rates: a case study,” *Rock Mechanics and Rock Engineering*, vol. 1, pp. 1–22, 2022.

[32] I. Jazayeri, C. Fraser, S. Cronk, I. Jazayeri, C. S. Fraser, and S. Cronk, *International Archives Of Photogrammetry, Remote Sensing and Spatial Information Sciences*, International Society for Photogrammetry and Remote Sensing, French, German, 2010.

[33] N. Snavely, S. M. Szeliski, and R. Szeliski, “Modeling the world from Internet photo collections,” *International Journal of Computer Vision*, vol. 80, no. 2, pp. 189–210, 2008.

[34] M. Favalli, A. Fornaciai, I. Isola, S. Nannipieri, and L. Nannipieri, “Multiview 3D reconstruction in geosciences,” *Computers & Geosciences*, vol. 44, pp. 168–176, 2012.

[35] M. R. Robson and S. Robson, “Straightforward reconstruction of 3D surfaces and topography with a camera: accuracy and geoscience application,” *Journal of Geophysical Research: Earth Surface*, vol. 117, no. F3, pp. a–n, 2012.

[36] P. Zou, X. Zhao, Z. Meng, A. Li, Z. Hu, and W. Hu, “Sample rocks tests and slope stability analysis of a mine waste dump,” *Advances in Civil Engineering*, vol. 2018, pp. 1–17, 2018.

[37] H. Lin, P. Cao, J. T. Li, X. L. Jiang, and Z. M. He, “Automatic generation of FLAC3D model based on SURPAC,” *Journal of China University of Mining and Technology*, vol. 37, no. 3, pp. 339–342, 2008.

[38] A. Kainthola, D. Verma, S. S. Singh, and T. N. Singh, “A coal mine dump stability analysis-A case study,” *Geomaterials*, vol. 1, no. 1, pp. 1–13, 2011.

[39] R. Chakravarty and D. Chakravarty, “Characterisation of overburden dump materials: a case study from the Wardha valley coal field,” *Bulletin of Engineering Geology and the Environment*, vol. 75, no. 3, pp. 1311–1323, 2016.

[40] W. K. Verma and A. K. Verma, “Probabilistic seismic hazard analysis for Kakrapar atomic power station, Gujarat, India,” *Natural Hazards*, vol. 69, no. 1, pp. 919–952, 2013.

[41] R. Chakravarty and D. Chakravarty, “Earthquake response of external mine overburden dumps: a micromechanical approach,” *Natural Hazards*, vol. 56, no. 3, pp. 941–959, 2011.

[42] J. Ji, W. Zhang, F. Zhang, Y. Lü, and Q. Lü, “Reliability analysis on permanent displacement of earth slopes using the simplified bishop method,” *Computers and Geotechnics*, vol. 117, Article ID 103286, 2020.

[43] R. Koner, “D.C.-A. in G.E. and undefined,” *Evaluation of Seismic Response of External Mine Overburden Dumps*, researchgate.net, 2010.

[44] R. Chakrabortty, S. C. Pal, S. Das, and B. Das, “Modeling and mapping of groundwater potentiality zones using AHP and GIS technique: a case study of Raniganj Block, Paschim Bardhaman, West Bengal,” *Modeling Earth Systems and Environment*, vol. 4, no. 3, pp. 1085–1110, 2018.

[45] A. K. Singh, M. K. Mahato, B. Singh, and K. K. Singh, “Quality assessment of mine water in the Raniganj coalfield area, India,” *Mine Water and the Environment*, vol. 29, no. 4, pp. 248–262, 2010.

[46] X. Fu, Q. Sheng, G. Li, Z. Zhang, Y. Du, and Y. Du, “Analysis of landslide stability under seismic action and subsequent rainfall: a case study on the Ganjiazhai giant landslide along the Zhaotong-Qiaojia road during the 2014 Ludian earthquake, Yunnan, China,” *Bulletin of Engineering Geology and the Environment*, vol. 79, no. 10, pp. 5229–5248, 2020.

[47] F. q. Tang, “Mining subsidence monitoring using the method of combining InSAR and GPS technology,” *Journal of Coal Science and Engineering*, vol. 17, no. 2, pp. 133–136, 2011.

[48] G. Erbach and D. C. Erbach, “Effect of wetting and drying on soil physical properties,” *Journal of Terramechanics*, vol. 36, no. 1, pp. 39–49, 1999.

[49] J. Ji, C. Zhang, Y. Kodikara, and J. Kodikara, “Reliability-based design for geotechnical engineering: an inverse FORM

approach for practice," *Computers and Geotechnics*, vol. 111, pp. 22–29, 2019.

[50] J. Ji, C. Zhang, Y. Kodikara, and J. Kodikara, "Effect of 2D spatial variability on slope reliability: a simplified FORM analysis," *Geoscience Frontiers*, vol. 9, no. 6, pp. 1631–1638, 2018.

[51] J. Ji, C. W. Wang, Y. Gao, and L. Zhang, "Probabilistic investigation of the seismic displacement of earth slopes under stochastic ground motion: a rotational sliding block analysis," *Canadian Geotechnical Journal*, vol. 58, pp. 952–968, 2021.